Title

A quantum chemistry study of curvature effects on boron nitride nanotubes/nanosheets for gas adsorption

Journal

Physical Chemistry Chemical Physics, 18(29)

ISSN

0956-5000

Authors

Sha, Haoyan
Faller, Roland

Publication Date

2016-07-20

DOI

10.1039/c6cp02540d

Peer reviewed

PCCP

PAPER

View Article Online
View Journal | View Issue

Cite this: *Phys. Chem. Chem. Phys.*, 2016, **18**, 19944

A quantum chemistry study of curvature effects on boron nitride nanotubes/nanosheets for gas adsorption†

Haoyan Sha and Roland Faller*

Received 15th April 2016,
Accepted 1st July 2016

DOI: 10.1039/c6cp02540d

www.rsc.org/pccp

Quantum chemistry calculations were performed to investigate the effect of the surface curvature of a Boron Nitride (BN) nanotube/nanosheet on gas adsorption. Curved boron nitride layers with different curvatures interacting with a number of different gases including noble gases, oxygen, and water on both their convex and concave sides of the surface were studied using density functional theory (DFT) with a high level dispersion corrected functional. Potential energy surfaces of the gas molecules interacting with the selected BN surfaces were investigated. In addition, the charge distribution and electrostatic potential contour of the selected BN surfaces are discussed. The results reveal how the curvature of the BN surfaces affects gas adsorption. In particular, small curvatures lead to a slight difference in the physisorption energy, while large curvatures present distinct potential energy surfaces, especially for the short-range repulsion.

Introduction

One- and two-dimensional layered nanostructured materials have attracted intense attention over the last two decades including nanotubes, nanosheets, nanoscrolls, *etc.*[1–10] Various inorganic elements and compounds have been explored for next generation layered nanomaterials, such as carbon, boron nitride, and silicon compounds. This novel class of materials possesses fascinating mechanical, thermal, and structural properties, and has enormous potential for real-world applications. Particularly, the high specific surface area proves excellent for gas adsorption and storage.[4,11] Well-defined nanoporous structures also show great potential for gas mixture separations.

Among layered nanostructured materials, graphene and carbon nanotubes are by far the best studied.[12] The adsorption properties have been systematically studied both experimentally and theoretically using quantum mechanics and molecular simulation methods. Many gas molecules, including H_2,[13–15] N_2,[16,17] methane,[18,19] noble gases,[20] and others as well as their mixtures, have been successfully investigated. Defects and packing effects on carbon surfaces were also studied.[21,22]

BN structures have been studied much less to date.[2] However, BN materials possess competitive thermal and structural stabilities with carbon making them excellent materials for gas adsorption.[23] Cheng *et al.* studied hydrogen physisorbed in single wall boron nitride nanotube (BNNT) bundles using the grand canonical Monte Carlo (GCMC) method.[24] Baierle *et al.* applied DFT to study the effect of carbon doping in BNNT on H_2 adsorption.[25] Zhao and Ding investigated gas molecules interacting with the open ends of BNNT.[26] Zhao *et al.* studied the non-covalent adsorption of aromatic molecules on BNNTs utilizing *ab initio* methods.[27] Shadman and Ahadi used GCMC for noble gases, argon and neon adsorbing in BNNTs.[28] A few comparative simulation studies were performed between BNNTs and CNTs on hydrogen adsorption and the DFT results present comparable capacities for H_2 storage where a controversy exists as Mpourmpakis and Froudakis state that BNNTs are more favorable than CNT for adsorbing H_2[29] while Zhou *et al.* state the opposite.[30] There is an insufficient understanding of gas adsorption on layered BN surfaces, particularly, how the surface curvature affects gas adsorption. Baierle *et al.*[25] and Mpourmpakis and Froudakis[31] studied the CNT curvature and chirality effects on adsorption using *ab initio* methods. However, to the best of our knowledge, the curvature effect on BN layered nanostructures on adsorption has not yet been investigated.

Here, density functional theory was applied to study the interactions between BN surfaces with different curvatures of different gases, including noble gases, O_2, and H_2O, which are representative monoatomic, diatomic and polyatomic molecules and important adsorbents of interest in a variety of applications. Potential energy surfaces were scanned on both the convex and concave sides of the selected surfaces. The effect of surface curvature on physisorption was analyzed by determining physisorption energy differences between curved and

Department of Chemical Engineering, University of California, Davis, Davis, CA, 95616, USA. E-mail: rfaller@ucdavis.edu; Tel: +1 530 752-5839

† Electronic supplementary information (ESI) available. See DOI: 10.1039/c6cp02540d

flat BN surfaces. The charge distributions, electrostatic potentials, and HOMO–LUMO orbitals of the selected BN surfaces were also discussed.

Model & methods

All boron nitride surfaces consist of 18 boron and 18 nitrogen atoms, with a B–N bond length of 1.446 Å. The flat BN surface was cut from a BN nanosheet (*cf.* Fig. 1(a)), while the curved ones (Fig. 1(b–e)) were taken from boron nitride nanotubes with indices of (5, 5), (10, 10), (15, 15), and (20, 20) respectively, which describe the sizes of the nanotubes, as shown in Table 1. The dangling bonds on the edges of the BN surfaces were satisfied with hydrogen atoms, with B–H and N–H bond lengths of 1.20 Å and 1.02 Å, respectively.[32] Utilizing the cluster model to represent the curved nanotube structure has been previously verified in the literature by modeling of materials in similar structures and presented excellent quality.[33–35]

The Gaussian code[36] was used for all DFT calculations[37,38] using the dispersion and long-range corrected wB97XD functional and the 6-311G(d,p) basis set.[39] Please note that according to the insufficiency of the quantum description of weak interatomic interactions by DFT[40] the purpose of this study is not to quantify the detailed potential energies of the gas with the BN surfaces with high accuracy. Instead, we study how the curvature of the BN surfaces affects gas adsorption at a consistent level and we kept all model parameters (except curvature) exactly the same across all studies.

The potential energy of physisorption was calculated by deducting the energy of the BN surface and the gas molecule from the energy of the BN–gas complex:

$$E_{\text{Physisorption}} = E_{\text{Complex}} - E_{\text{BN}} - E_{\text{Gas}}$$

Counterpoise correction was used to eliminate basis set superposition errors.[41,42] Potential energy surfaces (PESs) were studied by scanning gas molecules along the radial direction on convex and concave sides of the selected BN surfaces.

Table 1 Sizes of the curved BN surfaces

Index	Diameter of BNNT (Å)
(5, 5)	6.90
(10, 10)	13.81
(15, 15)	20.71
(20, 20)	27.62

Results and discussion

To determine the energetically most preferred binding site on the BN surface, three potential choices on a flat BN nanosheet were tested using a single argon atom. These positions are on top of boron, on top of nitrogen and on top of the center of the BN hexagon, as these are the symmetrically most likely candidates for the extrema. The corresponding PESs are plotted in Fig. 2. The three adsorption sites are not significantly different at large distances; at short distances the position on top of

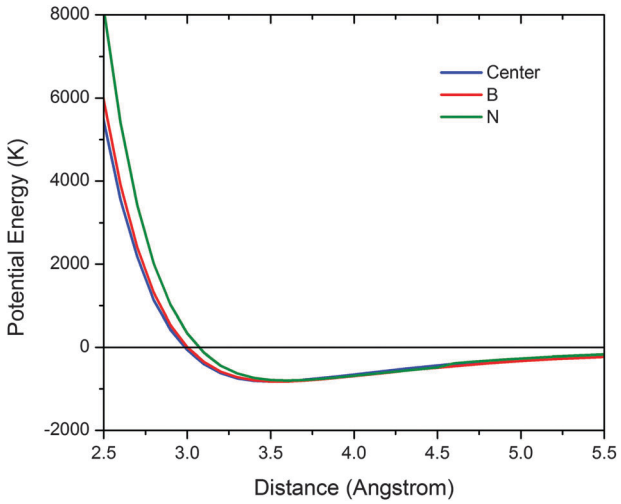

Fig. 2 Potential energy plots of argon binding towards nitrogen, boron, and the center of the BN hexagon.

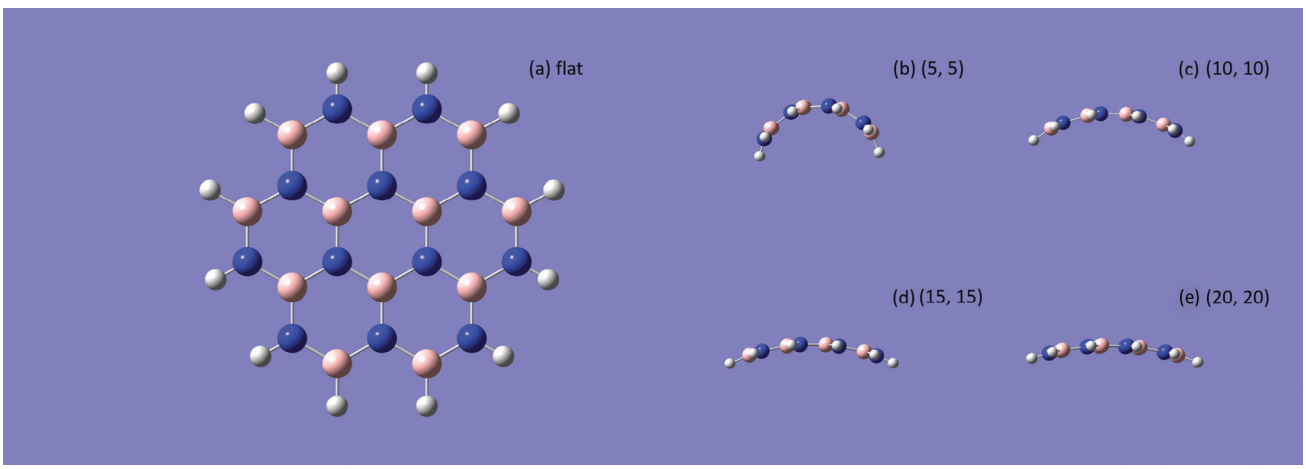

Fig. 1 Model of BN surfaces: (a) flat (top view); (b) (5, 5); (c) (10, 10); (d) (15, 15); and (e) (20, 20) (b–e side views). Blue: nitrogen; pink: boron; and white: hydrogen.

nitrogen faces stronger repulsion than the other two. The overall adsorption on top of the center of the hexagon is the energetically most favorable adsorption site. Therefore, all the following PES scans of gases above BN surfaces (flat/curved) were performed along the axis through the centers of the hexagons.

To evaluate the curvature effect on adsorption, noble gases which are highly symmetric and only slightly polarizable monoatomic structures were tested first. Fig. 3 shows PES and PES difference curves collected from an argon atom interacting with the BN sheet on both the convex and concave sides. The curvature influence on adsorption is characterized by the difference of adsorption energies between the curved BN surfaces and the flat surface:

$$E_{\text{Difference}} = E_{\text{Curved}} - E_{\text{Flat}}$$

The adsorption energy data are presented in Table 2. On the convex side of the surface (*cf.* Fig. 3(a and b)), the curvature only slightly changes the shape of the potential energy well, where the surface with stronger curvature presents a shallower energy well.

Table 2 Gas–BN surface adsorption energies

	Ar adsorption energy (K)		O_2 adsorption energy (K)	
BN surface	Convex side	Concave side	Convex side	Concave side
(5, 5)	−642.34752	−1277.5507	−488.03104	−1042.6102
(10, 10)	−706.53504	−1051.8918	−512.57056	−750.24416
(15, 15)	−735.62976	−957.72256	−529.54048	−683.08928
(20, 20)	−753.3744	−915.8416	−540.77952	−656.68352
Flat	−826.09568		−601.5264	

Only at short distances the curvature significantly affects the repulsion. For the flat surface at close approach the boron and nitrogen atoms closest to the approaching hexagon center lead to repulsion. However, the B and N atoms further from the adsorption site locate at attractive distances for the atom, which partially offsets the repulsion from the first ring. By increasing the curvature, the outer B and N atoms which show attraction on the flat surface are moved away from the adsorbent atom, so that the attraction from these atoms becomes weaker. The net potential then increases such that with larger curvature the short-distance repulsion increases.

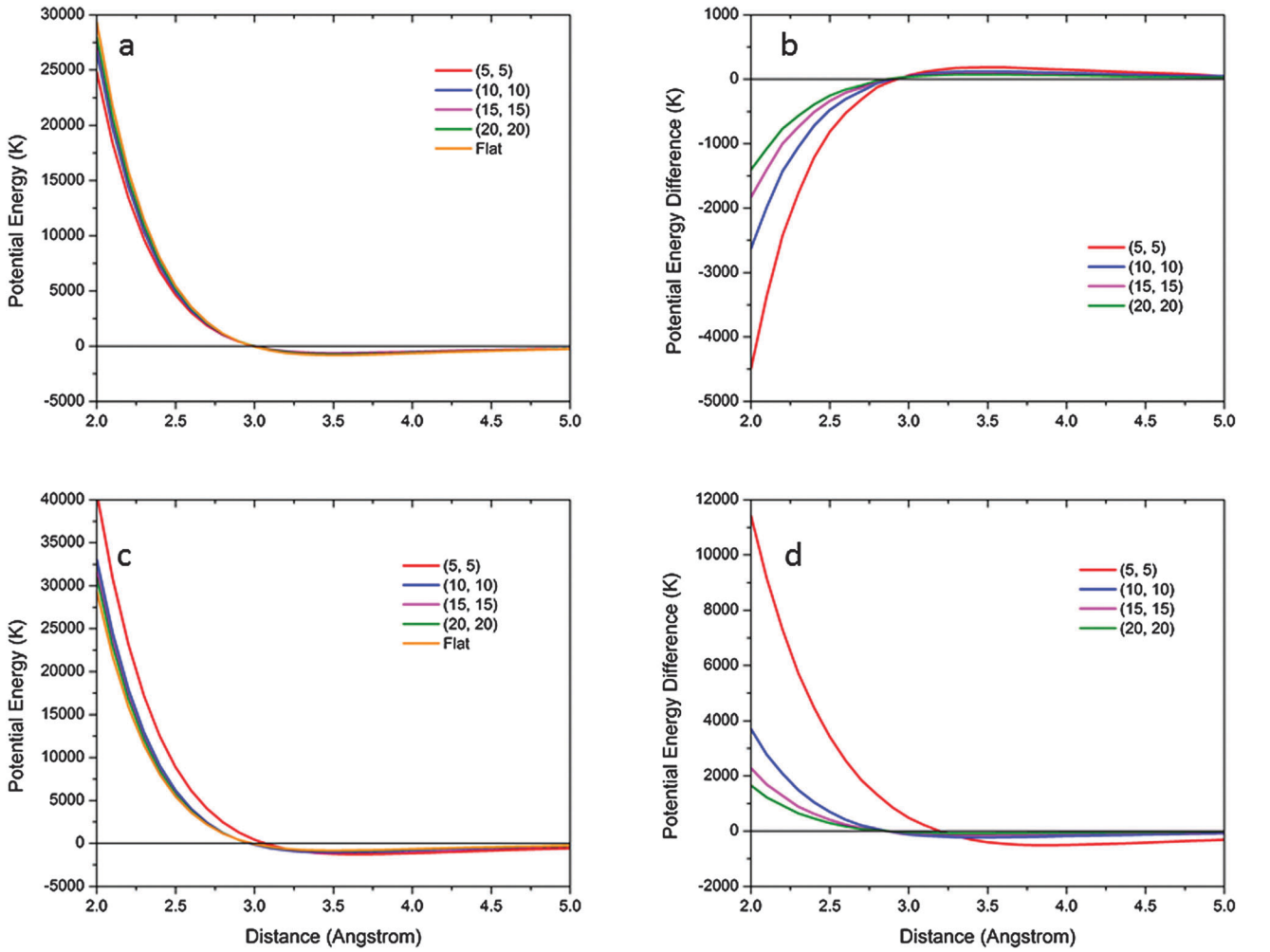

Fig. 3 Ar–BN surfaces: (a) convex side potential energy; (b) convex side potential energy difference; (c) concave side potential energy; and (d) concave side potential energy difference.

On the other hand, the concave sides of the BN surfaces show reversed trends of physisorption, where the larger curvature exhibits stronger attraction, which also is due to contributions from BN atoms at intermediate distance from the Ar atom. When the curvature becomes very high for the (5, 5) surface the Ar atom exhibits attraction at a much longer distance to the surface and the crossover from more repulsive to more attractive with respect to the flat surface is shifted outwards, so that the shape of the PES qualitatively changes leading to a confinement effect. Data of Ne–BN surface interactions consistent with these data can be found in the ESI,† Fig. S1.

In addition to noble gases, oxygen was tested for the curvature effect on adsorbate–adsorbent interaction. Oxygen was aligned with the oxygen–oxygen bond perpendicular to the surface. The corresponding PES data are plotted in Fig. 4. For the convex side, the oxygen, which has fewer electrons than argon, presents a weaker total adsorption and the adsorption energy changes with curvature consistent with the noble gases. For the concave side, more significant PES shape changes compared to noble gases are observed. The diatomic structure of oxygen provides an extra interaction site, which makes the confinement effect stronger for O_2. This has been further confirmed using H_2O PES data (ESI,† Fig. S2). The physisorption energies of all the selected gases are presented in Fig. S3 (ESI†), where we see that argon has the strongest interaction whereas the other three are in the same order of magnitude. Water has a steeper repulsion than oxygen and Ne.

The interaction strength differences between the selected adsorbents interacting with the BN surfaces are mainly caused by the different van der Waals and electrostatic potential energies. For non-polarized systems, the van der Waals interaction, which comes from the instantaneous dipole of the molecules, plays the most important role. van der Waals potential has a strong dependence on the atomic mass. That explains why argon has the strongest potential energy among the BN surfaces while the neon–BN interaction is the weakest. For polarized molecules, like H_2O, the unbalanced charge distribution causes strong electrostatic potential between H_2O and BN, which enables it stronger interaction with BN surfaces than molecular oxygen and neon.

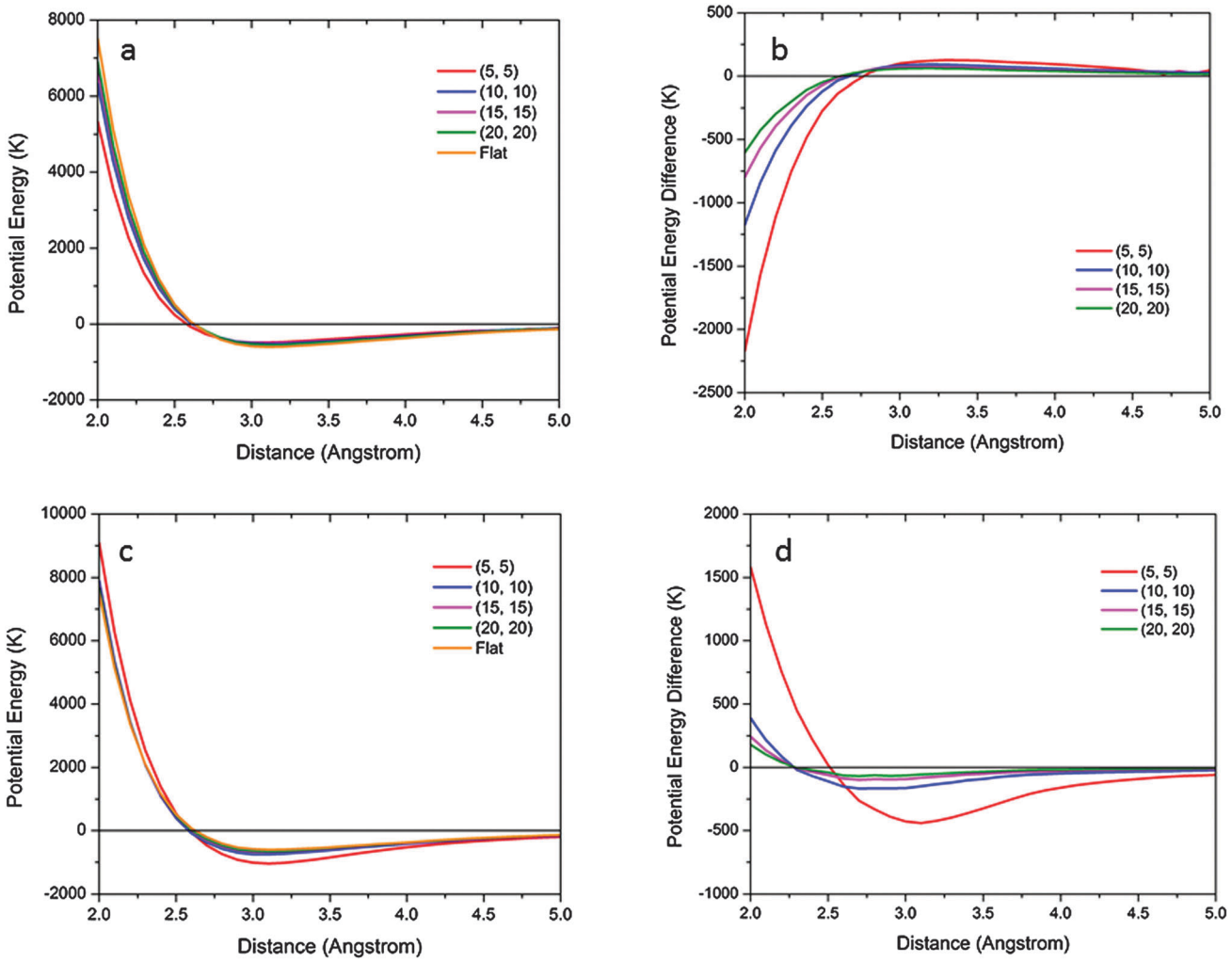

Fig. 4 O_2–BN surfaces: (a) convex side PES; (b) convex side potential energy difference; (c) concave side PES; and (d) concave side potential energy difference.

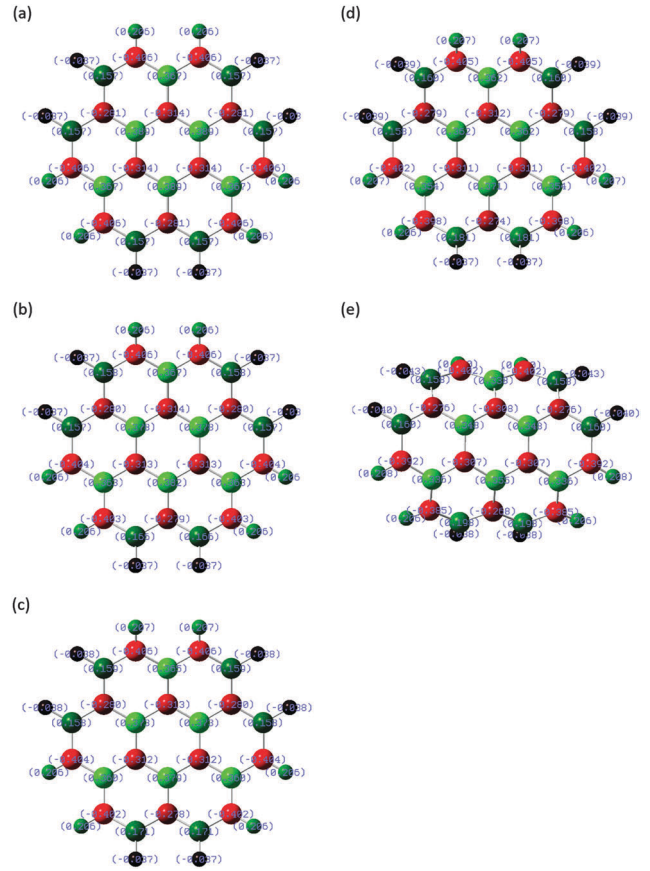

Fig. 5 BN surface charge distributions: (a) flat, (b) (20, 20), (c) (15, 15), (d) (10, 10), and (e) (5, 5). Color ranges from red to green representing elementary charges from −0.41 to 0.41 as labeled.

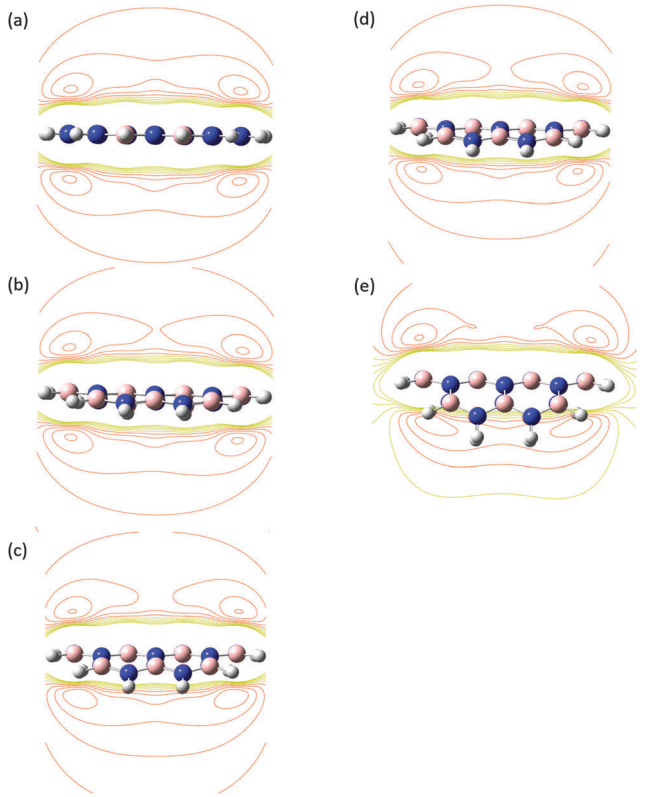

Fig. 6 Electrostatic potential (ESP) contours of the BN surfaces: (a) flat, (b) (20, 20), (c) (15, 15), (d) (10, 10), and (e) (5, 5). ESP iso-values were selected as 0.001, 0.003, 0.005, 0.007, and 0.009 a.u.

In addition to the PES analysis, the charge distributions and the corresponding electrostatic potential (ESP) contours of the flat and curved BN surfaces are shown in Fig. 5 and 6. With increasing curvature, the charges on the boron and nitrogen atoms do not significantly change, with only slightly reduced dipolarization. The corresponding ESP contours are plotted on the surface perpendicular to the BN sheets for the selected isosurfaces in Fig. 6. By introducing curvature, the symmetric ESP contour of the flat BN surface distorts. This distortion is also clearly visible in the HOMO and LUMO orbitals of the sheets (ESI,† Fig. S4 and S5) where one sees *e.g.* that the HOMO orbitals start to align with the central axis of the cylinder on which the sheet is based.

Conclusions

The present density functional theory study investigated the curvature effect on the example of layered boron nitride on gas adsorption. The selected gas molecules including noble gases (argon and neon), oxygen, and water were tested by scanning the gas–BN physisorption energy. Charge distribution and ESP of the BN surfaces were analysed. The results show that the curvature of the BN surface strengthens the short-distance repulsion on the convex side and increases the whole-range attraction on the concave side. Strong curvatures can significantly change the adsorption PES.

Acknowledgements

We acknowledge many helpful discussions with Dr Pieter Stroeve, Dr Ricardo Castro, and Dr Joe Tringe (LLNL). This research was supported by the U.S. Department of Energy, Office of Nuclear Energy, under Grant No. DE-NE0000704.

References

1 P. Ajayan, *Chem. Rev.*, 1999, **99**, 1787–1800.
2 D. Golberg, Y. Bando, Y. Huang, T. Terao, M. Mitome, C. Tang and C. Zhi, *ACS Nano*, 2010, **4**, 2979–2993.
3 S. Iijima, *Physica B*, 2002, **323**, 1–5.
4 R. E. Morris and P. S. Wheatley, *Angew. Chem., Int. Ed.*, 2008, **47**, 4966–4981.
5 Y. Lin and J. W. Connell, *Nanoscale*, 2012, **4**, 6908–6939.
6 S. F. Braga, V. R. Coluci, S. B. Legoas, R. Giro, D. S. Galvão and R. H. Baughman, *Nano Lett.*, 2004, **4**, 881–884.
7 P. Eric and S. G. Douglas, *Nanotechnology*, 2009, **20**, 335702.
8 D. Golberg, Y. Bando, C. C. Tang and C. Y. Zhi, *Adv. Mater.*, 2007, **19**, 2413–2432.
9 J. Lu, S. Nagase, X. Zhang, D. Wang, M. Ni, Y. Maeda, T. Wakahara, T. Nakahodo, T. Tsuchiya, T. Akasaka,

Z. Gao, D. Yu, H. Ye, W. N. Mei and Y. Zhou, *J. Am. Chem. Soc.*, 2006, **128**, 5114–5118.
10 W. An, X. Wu and X. C. Zeng, *J. Phys. Chem. C*, 2008, **112**, 5747–5755.
11 Q. Weng, X. Wang, C. Zhi, Y. Bando and D. Golberg, *ACS Nano*, 2013, **7**, 1558–1565.
12 M. J. Allen, V. C. Tung and R. B. Kaner, *Chem. Rev.*, 2010, **110**, 132–145.
13 J. Cheng, X. Yuan, L. Zhao, D. Huang, M. Zhao, L. Dai and R. Ding, *Carbon*, 2004, **42**, 2019–2024.
14 Z. Ahadi, M. Shadman, S. Yeganegi and F. Asgari, *J. Mol. Model.*, 2011, **18**, 2981–2991.
15 M. Shadman, S. Yeganegi and M. R. Galugahi, *J. Iran. Chem. Soc.*, 2015, **13**, 207–220.
16 J. Jiang and S. I. Sandler, *Langmuir*, 2004, **20**, 10910–10918.
17 J. Jiang and S. I. Sandler, *Phys. Rev. B: Condens. Matter Mater. Phys.*, 2003, **68**, 245412.
18 M. Bienfait, P. Zeppenfeld, N. Dupont-Pavlovsky, M. Muris, M. R. Johnson, T. Wilson, M. DePies and O. E. Vilches, *Phys. Rev. B: Condens. Matter Mater. Phys.*, 2004, **70**, 035410.
19 M. Muris, N. Dufau, M. Bienfait, N. Dupont-Pavlovsky, Y. Grillet and J. P. Palmari, *Langmuir*, 2000, **16**, 7019–7022.
20 H. Sha and R. Faller, *Comput. Mater. Sci.*, 2016, **114**, 160–166.
21 M. R. LaBrosse and J. K. Johnson, *J. Phys. Chem. C*, 2010, **114**, 7602–7610.
22 M. R. LaBrosse, W. Shi and J. K. Johnson, *Langmuir*, 2008, **24**, 9430–9439.
23 M. Won Ha and H. Ho Jung, *Nanotechnology*, 2004, **15**, 431.
24 J. Cheng, L. Zhang, R. Ding, Z. Ding, X. Wang and Z. Wang, *Int. J. Hydrogen Energy*, 2007, **32**, 3402–3405.
25 R. J. Baierle, P. Piquini, T. M. Schmidt and A. Fazzio, *J. Phys. Chem. B*, 2006, **110**, 21184–21188.
26 J.-X. Zhao and Y.-H. Ding, *J. Phys. Chem. C*, 2008, **112**, 20206–20211.
27 Y. Zhao, X. Wu, J. Yang and X. Cheng Zeng, *Phys. Chem. Chem. Phys.*, 2011, **13**, 11766–11772.
28 M. Shadman and Z. Ahadi, *Fullerenes, Nanotubes, Carbon Nanostruct.*, 2011, **19**, 700–712.
29 G. Mpourmpakis and G. E. Froudakis, *Catal. Today*, 2007, **120**, 341–345.
30 Z. Zhou, J. Zhao, Z. Chen, X. Gao, T. Yan, B. Wen and P. V. R. Schleyer, *J. Phys. Chem. B*, 2006, **110**, 13363–13369.
31 G. Mpourmpakis, G. E. Froudakis, G. P. Lithoxoos and J. Samios, *J. Chem. Phys.*, 2007, **126**, 144704.
32 O. Hod, *J. Chem. Theory Comput.*, 2012, **8**, 1360–1369.
33 J. Lan, D. Cheng, D. Cao and W. Wang, *J. Phys. Chem. C*, 2008, **112**, 5598–5604.
34 G. Mpourmpakis, G. E. Froudakis, G. P. Lithoxoos and J. Samios, *Nano Lett.*, 2006, **6**, 1581–1583.
35 M. K. Kostov, E. E. Santiso, A. M. George, K. E. Gubbins and M. B. Nardelli, *Phys. Rev. Lett.*, 2005, **95**, 136105.
36 M. J. Frisch, G. W. Trucks, H. B. Schlegel, G. E. Scuseria, M. A. Robb, J. R. Cheeseman, G. Scalmani, V. Barone, B. Mennucci, G. A. Petersson, H. Nakatsuji, M. Caricato, X. Li, H. P. Hratchian, A. F. Izmaylov, J. Bloino, G. Zheng, J. L. Sonnenberg, M. Hada, M. Ehara, K. Toyota, R. Fukuda, J. Hasegawa, M. Ishida, T. Nakajima, Y. Honda, O. Kitao, H. Nakai, T. Vreven, J. A. Montgomery, Jr., J. E. Peralta, F. Ogliaro, M. Bearpark, J. J. Heyd, E. Brothers, K. N. Kudin, V. N. Staroverov, R. Kobayashi, J. Normand, K. Raghavachari, A. Rendell, J. C. Burant, S. S. Iyengar, J. Tomasi, M. Cossi, N. Rega, J. M. Millam, M. Klene, J. E. Knox, J. B. Cross, V. Bakken, C. Adamo, J. Jaramillo, R. Gomperts, R. E. Stratmann, O. Yazyev, A. J. Austin, R. Cammi, C. Pomelli, J. W. Ochterski, R. L. Martin, K. Morokuma, V. G. Zakrzewski, G. A. Voth, P. Salvador, J. J. Dannenberg, S. Dapprich, A. D. Daniels, Ö. Farkas, J. B. Foresman, J. V. Ortiz, J. Cioslowski and D. J. Fox, *Gaussian 09*, Gaussian, Inc., Wallingford CT, 2009.
37 D. Frenkel and B. Smit, *Understanding Molecular Simulation*, Elsevier, Singapore, 2010.
38 F. Jensen, *Introduction to Computational Chemistry*, John Wiley & Sons, 2006.
39 J.-D. Chai and M. Head-Gordon, *Phys. Chem. Chem. Phys.*, 2008, **10**, 6615–6620.
40 Y. Andersson, E. Hult, H. Rydberg, P. Apell, B. Lundqvist and D. Langreth, in *Electronic Density Functional Theory*, ed. J. Dobson, G. Vignale and M. Das, Springer, US, 1998, ch. 17, pp. 243–260, DOI: 10.1007/978-1-4899-0316-7_17.
41 S. F. Boys and F. Bernardi, *Mol. Phys.*, 1970, **19**, 553–566.
42 H. B. Jansen and P. Ros, *Chem. Phys. Lett.*, 1969, **3**, 140–143.